Biophysics

Volume 2, Issue 3, 381-397.
DOI: 10.3934/biophy.2015.3.381
Received date 15 May 2015,
Accepted date 20 August 2015,
Published date 31 August 2015

http://www.aimspress.com/

Research article

Regulation of Aquaporin Z osmotic permeability in ABA tri-block copolymer

Wenyuan Xie [1], Jason Wei Jun Low [1], Arunmozhiarasi Armugam [2], Kandiah Jeyaseelan [2], and Yen Wah Tong [1,3,*]

[1] NUS Environmental Research Institute (NERI), National University of Singapore #02-01, T-Lab Building 5A Engineering Drive 1, Singapore 117411
[2] Department of Biochemistry, Yong Loo Lin School of Medicine, National University of Singapore, 8 Medical Drive, Singapore 117597
[3] Department of Chemical and Biomolecular Engineering, National University of Singapore, 4 Engineering Drive 4, Singapore 117585

* **Correspondence:** Email: chetyw@nus.edu.sg; Tel: +65-65168467; Fax: +65-67791936.

Abstract: Aquaporins are transmembrane water channel proteins present in biological plasma membranes that aid in biological water filtration processes by transporting water molecules through at high speeds, while selectively blocking out other kinds of solutes. Aquaporin Z incorporated biomimetic membranes are envisaged to overcome the problem of high pressure needed, and holds great potential for use in water purification processes, giving high flux while keeping energy consumption low. The functionality of aquaporin Z in terms of osmotic permeability might be regulated by factors such as pH, temperature, crosslinking and hydrophobic thickness of the reconstituted bilayers. Hence, we reconstituted aquaporin Z into vesicles that are made from a series of amphiphilic block copolymers PMOXA-PDMS-PMOXAs with various hydrophobic molecular weights. The osmotic permeability of aquaporin Z in these vesicles was determined through a stopped-flow spectroscopy. In addition, the temperature and pH value of the vesicle solutions were adjusted within wide ranges to investigate the regulation of osmotic permeability of aquaporin Z through external conditions. Our results show that aquaporin Z permeability was enhanced by hydrophobic mismatch. In addition, the water filtration mechanism of aquaporin Z is significantly affected by the concentration of H^+ and OH^- ions.

Keywords: aquaporin Z; biomimetic membranes; osmotic permeability; pH; hydrophobic mismatch

1. Introduction

Current membrane technologies are important in many industrial separation processes, especially in water purification and desalination. However, the large operating pressure gradient that is required for conventional reverse osmosis filtration makes water purification a very expensive process [1–4]. The discovery of aquaporin proteins has provided us with a revolutionary alternative to current membranes used in water purification.

Aquaporins (Aqp) are transmembrane proteins that are present in the biological membranes of organisms such as plants, mammals and bacteria [5,6]. They form pores that act as water channels, which play key roles in selectively allowing only water molecules to move across the plasma membrane while rejecting protons, charged particles and other solutes [7,8]. Aquaporin Z (AqpZ) is of special interest in water purification and seawater desalination. This is because AqpZ has been successfully expressed in *Escherichia coli* as reported by Soupene et al. [9], and has been purified in high concentrations to be used for integration into biomimetic membranes for water filtration [10,11]. Furthermore, AqpZ is the smallest, simplest and most robust aquaporin in the Aqp family and it can retain its properties after reconstitution in polymeric bilayer membrane vesicles [12].

Similar to other aquaporins, AqpZ naturally exists as a tetramer made up of 4 equal sub-units (or monomers) [13], with each aquaporin monomer having six transmembrane α-helical structures and five connecting loops named A to E [12]. Each aquaporin monomer contains an individual pore, or water channel, that allows the transport of water bi-directionally with water transport rates of up to 10^9 molecules per second. Loops B and E contain the most highly conserved residues, including the asparagine–proline–alanine (NPA) signature motif of Aqp, which are directly involved in the water channel function of Aqp. Loops B and E fold into the membrane from opposite sides of the bilayer, overlapping midway through the bilayer where they are surrounded by six transmembrane helices, forming the "hour-glass" model of the water channel. Owing to its unique hour-glass configuration with the NPA motif, AqpZ is capable of achieving high water selectivity and 100% salt rejection. Three features of the water channel contribute to this high selectivity for water, which are size restriction, electrostatic repulsion and water dipole re-orientation [13]. Firstly, the narrowest constriction of the pore has a diameter of 2.8 Å [13], which is approximately the diameter of a water molecule. Hence, water molecules are physically sieved through and allowed to penetrate while other ions and solutes are rejected due to this selective property. Another feature contributing to the high water selectivity of aquaporin is the electrostatic repulsion induced by one of the conserved residue, Arg-195, located at the narrowest pore constriction [13–16]. This residue carries a strong positive charge which repels cations including protonated water, H_3O^+, hence preventing the passage of positively-charged ions. The third feature is that the hemipore loops carrying the NPA motifs—Loops B and E—form helices that meet midway of the channel, producing positively charged dipoles that reorient water molecules. This water dipole reorientation results in the opposite alignment of water molecules, which disrupts hydrogen bonding between neighbouring water molecules. Hence, the conductance of H^+ ions is eliminated [17].

In most Aqp, the hydrophobic channels function as open channels, but some plant aquaporins, such as the spinach Aqp, have been described by Chaumont et al. (2005) to exhibit a form of gating mechanism. These Aqp are able to close up their channels under extreme conditions in order to stop water exchange altogether, which lends credence to the basis that AqpZ permeability is likely to vary with external conditions, even though they may or may not exhibit the same form of gating mechanisms observed [18]. However, the water filtration mechanisms by which these Aqp function are not fully understood. The protein will be influenced by external factors such as pH and

temperature, which can cause a disruption to its structure and affect the protein's functionality and properties [19]. The different external conditions can induce structural changes of the Aqp proteins and may lead to an adverse or favorable effect on the water transport and selection mechanism. Hence, it may result in a change to the osmotic permeability of AqpZ.

In addition, the thickness of the phospholipid bilayer may regulate transmembrane proteins funcationalities due to the hydrophobic mismatch between the hydrophobic length of the transmembrane proteins and the hydrophobic thickness of the bilayers [20–26]. To counteract the hydrophobic mismatch, either the surrounding bilayer thickness or the protein conformation will change, for example resulting in an activity change of melibiose tranporters or mechanosensitive ion channels [20–26]. To date, it remains unclear how the osmotic permeability of AqpZ will be affected by the hydrophobic thickness of the surrounding bialyer membrane.

Compared to phospholipids, amphiphilic block copolymers are more suitable in the fabrication of AqpZ reconstituted biomimetic membranes for the purpose of water filtration because block copolymers possess higher chemical and mechanical stability due to their chemical structures and flexible functional designs. ABA block copolymer, such as poly(2-methyloxazoline)-*b*-poly(dimethylsiloxane)-*b*-poly(2-methyloxazoline) (PMOXA-PDMS-PMOXA), has been widely used in fabrication of AqpZ-based biomimetic membrane for water purification [1,27–31]. It has been reported that the permeability of an AqpZ-reconstituted PMOXA-PDMS-PMOXA membrane is 167 μm/s/bar, which is by two orders of magnitude greater than commercial polymeric membranes [1]. Therefore, we chose the amphiphilic block copolymer of PMOXA-PDMS-PMOXAs as the bilayer matrix for AqpZ reconstitution in this work.

The rationale of the present study is to gain further insight into the regulation of AqpZ permeability through environmental conditions, including the protein-bilayer hydrophobic mismatch, pH and temperature. We reconstituted AqpZ into vesicles that are made from a series of amphiphilic block copolymers of PMOXA-PDMS-PMOXA with various hydrophobic molecular weights. The osmotic permeability of AqpZ in these vesicles is determined by stopped-flow spectroscopy. In addition, the temperature and pH of the vesicle solutions were adjusted within wide ranges to investigate the regulation of osmotic permeability of the AqpZ at different external conditions.

2. Materials and Methods

2.1. Expression and purification of Aquaporin Z

Aquaporin Z has been prepared as reported by Calamita et al. [6] and in our previous studies [27–31]. Briefly, *E. coli* genomic DNA was extracted and the *aqpZ* gene was amplified and cloned into the pCR-4 vector using the TOPO cloning kit (Invitrogen, USA). The positive clones were sequenced and further subcloned into a modified expression vector, the pQE-30 Xa expression vector, with ampicillin selection and an amino-terminal 10x His-affinity tag (Qiagen, USA). The *E. coli* strain TOP10F was transformed and grown to 0.6–1 OD at 600 nm in LB with 100 mg/l of ampicillin and subsequently induced with 1 mM of isopropyl-D-thiogalactoside. The harvested cells were resuspended in one 1/50 culture volume of ice-cold lysis buffer containing 100 mM of K_2HPO_4, 1 mM of $MgSO_4$, 1 mM of phenylmethylsulfonylfluoride (PMSF), and 0.1 mg/ml of deoxyribonuclease I (pH 7.0). Cells were subjected to 4 lysis cycles in a French press (115×10^6 Pa at 4 °C). The unbroken cells and debris were separated from the cell lysate by centrifugation at 10,000 *g* and discarded. Membrane fractions were recovered from the supernatant by centrifugation at 100,000 *g*. AqpZ was solubilized from pellets by agitation in 1% dodecyl maltoside and PBS [12].

The solubilized protein was purified through Ni–NTA resin (Qiagen, USA), washed, and eluted with PBS (pH 7.4) and 250 mM of imidazole. The imidazole was removed using a Bio-Rad (Hercules, California, United States) Econo-Pac DG10 desalting column [32]. The resulting recombinant Aquaporin Z protein contained the 10 His-tag at the protein's N-terminus and was utilized for embedding into membranes and vesicles.

2.2. ABA triblock copolymers

A series of ABA triblock copolymers, poly(2-methyloxazoline)-block-poly(dimethylsiloxane)-block-poly(2-methyloxazoline) (PMOXA-PDMS-PMOXA, Polymer Source Inc.), with various hydrophobic/hydrophilic compositions are used for AqpZ reconstitution, as shown in Table 1.

Table 1. ABA triblock copolymers used for preparation of AqpZ reconstituted vesicles.

Name	ABA triblock copolymers	Hydrophobic molecular weight of the polymer (Da.)	$f_{hydrophilic}$ (Hydrophilic mass ratio)
P_{2500} [a]	$PMOXA_{500}$-$PDMS_{2500}$-$PMOXA_{500}$ [c]	2500	28.57 %
P_{4000} [b]	$PMOXA_{1000}$-$PDMS_{4000}$-$PMOXA_{1000}$ [c]	4000	33.33 %
P_{5000} [b]	$PMOXA_{1300}$-$PDMS_{5000}$-$PMOXA_{1300}$ [c]	5000	34.21 %
P_{8500} [a]	$PMOXA_{1300}$-$PDMS_{8500}$-$PMOXA_{1300}$ [c]	8500	23.40 %
P_{8800} [a]	$PMOXA_{2000}$-$PDMS_{8800}$-$PMOXA_{2000}$ [c]	8800	31.25%

[a] tri-block copolymers P_{2500}, P_{8500} and P_{8800} are with hydroxyl end groups;

[b] tri-block copolymers P_{4000} and P_{5000} are with methacrylate end groups which allow for a UV light induced polymerization;

[c] In "$PMOXA_{xxx}$-$PDMS_{xxxx}$-$PMOXA_{xxx}$", the number after each block represents the molecular weight (Da.) of each block.

2.3. Preparation of blank polymer vesicles and AqpZ-reconstituted polymer vesicles

The blank copolymer vesicles were prepared using the film rehydration method shown in Figure 1. Each kind of polymer (3 mg) was dissolved in chloroform (5 ml) in a round bottomed flask. Chloroform was then evaporated slowly in a rotary vacuum evaporator at −10°C and at a vacuum of 400 mbar, to form an even and thin film of polymer at the bottom of the flask. The residual chloroform was further removed using a vacuum pump. The film was then rehydrated by the respective pH buffer (prepared from sodium chloride with hydrogen chloride or sodium hydroxide, with total ion concentration of 0.2 mol/L) solutions or deionized water, forming suspension with polymer concentration of 1 mg/ml. The mixture was left at room temperature with stirring for 10 h. The resultant polymersome suspension was extruded 21 times with a polycarbonate membrane with

pore diameter of 200 nm to achieve unilamellar vesicles with a narrow size distribution.

The preparation procedure for proteopolymersomes was similar as above. The only difference was in the reconstitution experiments, where an appropriate amount of AqpZ solution (1 mg/ml in 2% DDM (dodecyl maltoside) was added to the samples during rehydration. The detergent was removed by adding bio-beads into the mixture. The bio-beads were added every 4 h for 5 times, to allow for the adsorption process to reach equilibrium each time before the next batch of bio-beads adding into the suspension. Bio-beads were added in 5-fold excess in the last batch to ensure that the remaining detergent molecules will be adsorbed and removed entirely. The proteopolymersomes were then extruded with the same method as in the preparation of the blank polymersomes.

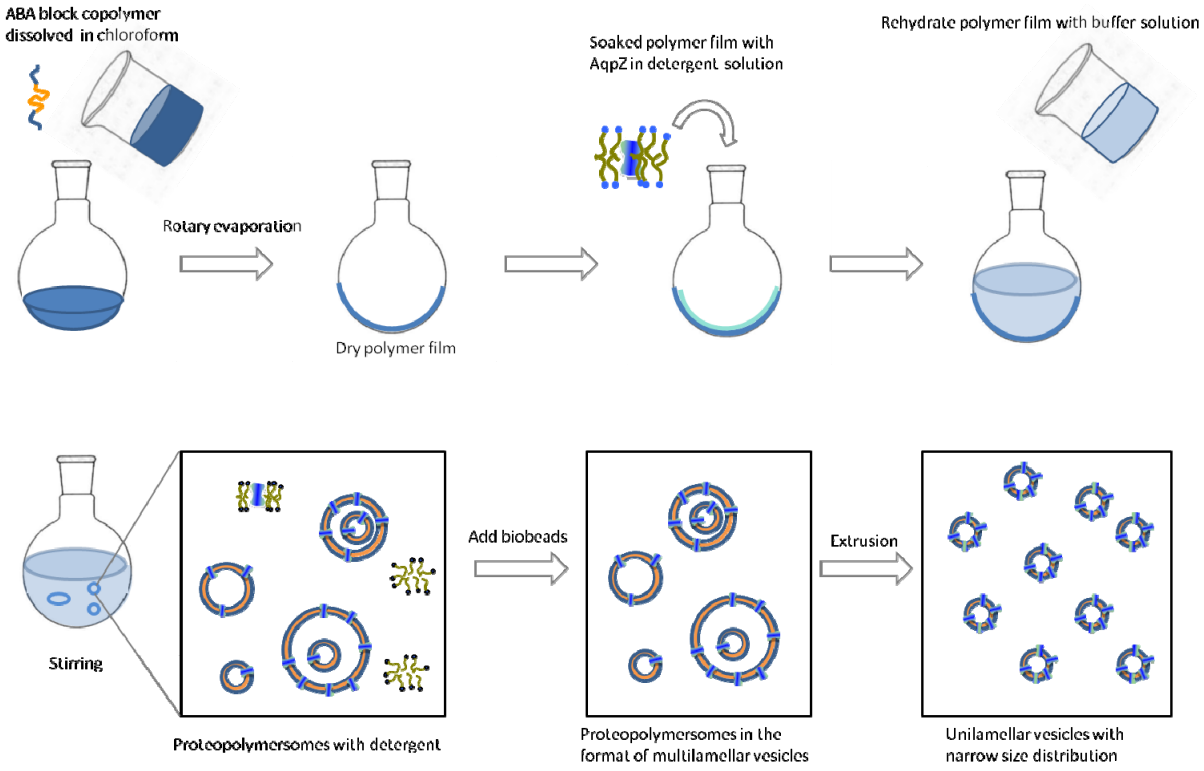

Figure 1. Schematic diagram for reconstitution of AqpZ into vesicles that are made from amphiphilic block copolymers.

2.4. UV-crosslinking of polymer vesicles

The extruded P_{4000} and P_{11500} polymersome suspensions were purged with argon for 10 min and further crosslinked under UV irradiation (254 nm, 6 mW cm^{-2}) for 15 min using a BLX-E254 crosslinker (Vilber Lourtmat, France). The polymer vesicles before and after UV irradiation were freeze-dried and characterized using a Fourier transform infrared spectrometer (FTIR-8400 Shimadzu Corp., Japan) to determine the crosslinking reaction between the methacrylate groups.

2.5. Size and morphology characterization of polymersomes

Vesicle size was measured by a dynamic light scattering unit (Zetasizer 3000 HAS equipped with a He–Ne laser beam at 658 nm, Malvern Instruments Ltd., Malvern, UK; scattering angle: 90°).

Vesicle suspensions were diluted to 0.01 mg/ml with DI water or respective buffer solution for the dynamic light scattering tests. An average value was obtained from three measurements.

Vesicle morphologies were measured using field emission transmission electron microscopy (FETEM), whereby the vesicles were stained on plasma-treated copper grids using 1% trifluoroacetic acid.

2.6. Characterization of permeability coefficient (Pf) of vesicles, permeability of reconstituted aquaporin Z (Pa) and the Arrhenius activation energy (Ea) of water molecules across polymer vesicles

The permeability coefficients of various polymer vesicles with or without AqpZ reconstitution were characterized using the stopped-flow (Chirascan Circular Dichroism Spectrometer, Applied Photophysics, UK) method. For each individual stopped-flow test, 0.13 ml extruded polymersome or proteopolymersome solution with polymer concentration of 1 mg/ml was quickly mixed with 0.13 ml sucrose buffer (0.6 osmol/L), which caused water efflux from vesicles that resulted in vesicle shrinkage. At least 6 tests were performed for each sample. The dead time for the mixing of stopped flow injection was 4 ms. The vesicle size changes were monitored and recorded in the form of an increasing signal in the light scattering analysis. The initial rise of the signal curve was fitted to equation (1).

$$Y = A\exp(-kt) \qquad (1)$$

Where Y is the signal intensity, A is the negative constant, k is the initial rate constant (s^{-1}), and t is the recording time. The osmotic water permeability was calculated using Equation (2).

$$P_f = \frac{k}{(S/V_0)V_w\Delta_{osm}} \qquad (2)$$

Where P_f is the osmotic water permeability (m/s), S is the vesicle surface area (m^2), V_0 is the initial vesicle volume (m^3), V_w is the partial molar volume of water (0.018 L/mol), and Δosm is the osmolarity difference that drives the shrinkage of the vesicles (osmol/L).

Single AqpZ channel permeability was calculated using Equation (3) [33].

$$P_a = \frac{P_{f,proteopolymersome} - P_{f,polymersome}}{Mon/A} \qquad (3)$$

$P_{f,proteopolymersome}$ is the permeability of the AqpZ-vesicles, $P_{f,polymersome}$ is the permeability of the polymersomes without AqpZ reconstitution, and Mon/A is the number of AqpZ monomers per unit area in the proteopolymersomes.

To measure the Arrhenius activation energy of water molecules across polymer vesicles, Stopped-flow experiments were carried out at different temperatures (5, 10, 15, 20, 25 and 30 °C) for both blank polymer vesicles and AqpZ-reconstituted polymer vesicles. The exponential increase rates (k) calculated from the light scattering signals were plotted against the inverse of temperature for calculation of the Arrhenius activation energies. The comparative experiments were all tested at room temperature.

2.7. Statistical analysis

All the data presented in this study represent the mean ± standard deviation values of three experiments, unless stated otherwise. Statistical differences between groups were found using a Student's t-test.

3. Results and Discussion

In this study, detailed investigation was carried out on the mechanism of water transport through AqpZ reconstituted polymer bilayers. Our aim was to establish a relationship between membrane matrix properties and the AqpZ functionality, as well as the relationship between the AqpZ permeability and the environmental conditions. Triblock copolymer PMOXA-PDMS-PMOXA is the most commonly used membrane matrix for AqpZ incorporation. The molecular structure including molecular weight, hydrophilic-lipophilic balance, functional end group and crosslinking capability, has to be considered carefully to ensure the successful incorporation of aquaporins into the vesicles to maintain its structure and function. We incorporated AqpZ into a series of PMOXA-PDMS-PMOXA block copolymers, adjusted the pH value of vesicle solutions, and controlled the temperature during stopped flow measurement, in order to investigate the influence of molecular structure of the membrane matrix and the external conditions on the osmotic permeability of the reconstituted AqpZ.

3.1. Block copolymer composition vs. vesicle formation and morphology

Amphiphilic block copolymers have similar behaviour as lipids, which are also amphiphilic. In aqueous solutions, amphiphilic block copolymers will self-assemble into various ordered morphologies, such as micelles, vesicles and lamellar phases. Three parameters of block copolymers play important roles in the phase transition between these morphologies, including the molecular weight of the polymer, the mass fraction (f) of each block, and the effective interaction energy between the repeating units in the blocks [34]. PMOXA-PDMS-PMOXA has been widely adopted to form vesicle bilayers for the reconstitution of transmembrane proteins [1,27,29] through self-assembly. In this section, we systematically investigated how the polymer molecular weight and the mass fraction of each block influence the self-assembly, and how the molecular weight of the hydrophobic block effects the AqpZ permeability.

A series of block copolymers PMOXA-PDMS-PMOXA with various molecular weight and hydrophobic/hydrophilic ratio were chosen to prepare proteopolymersomes, as listed in Table 1. The hydrophilic ratio ($f_{hydrophilic}$) of these polymers ranges from 23.4 to 34.2% in the sequence of $P_{8500} < P_{2500} < P_{8800} < P_{4000} < P_{5000}$. Figure 2 shows the morphologies of the self-assemblies without extrusion. It can be seen that all of them form vesicles except for P_{8500}. This result is consistent with previous report in that the $f_{hydrophilic}$ range of block copolymer to form vesicles is between 25 to 40% [35]. With increasing $f_{hydrophilic}$, vesicle size decreases sequentially as $P_{2500} > P_{8800} > P_{4000} > P_{5000}$. According to the simulation results from our previous work, larger vesicles are preferable since larger vesicles will generate higher water flux as compared to smaller ones in an AqpZ-incorporated-vesicular membrane [27]. Therefore, block copolymers with $f_{hydrophilic}$ ranging from 25 to 30% are preferable for preparation of AqpZ-incorporated-vesicular membrane.

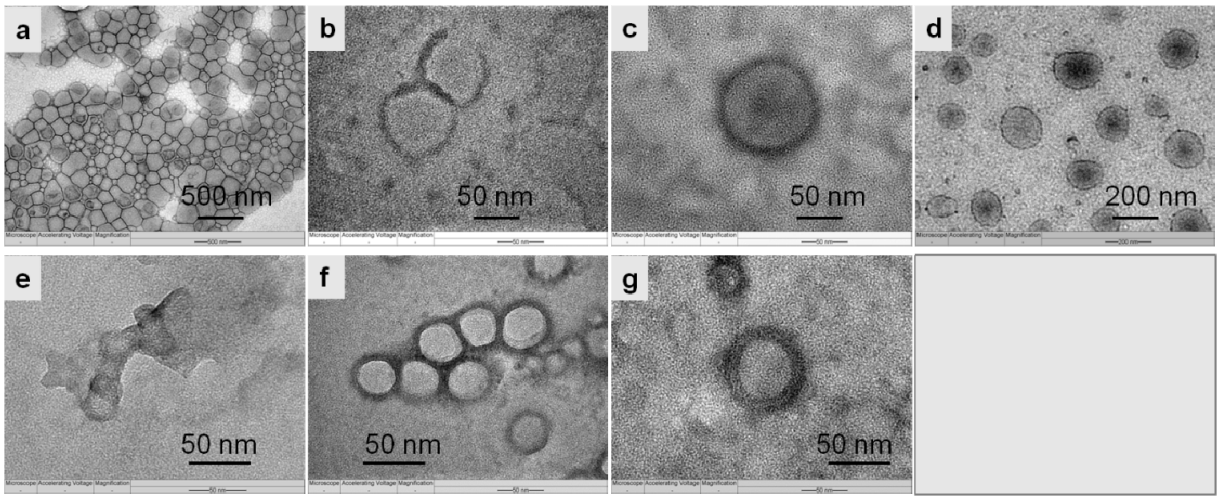

Figure 2. Morphologies of polymersomes by transmission electron microscope (TEM). Polymersomes are made from PMOXA-PDMS-PMOXAs with various molecular weights: (a) P_{2500}; (b) P_{4000}; (c) P_{4000} after exposure to UV irradiation; (d) P_{8800}; (e) P_{8500}; (f) P_{5000}; (g) P_{5000} after exposure to UV irradiation.

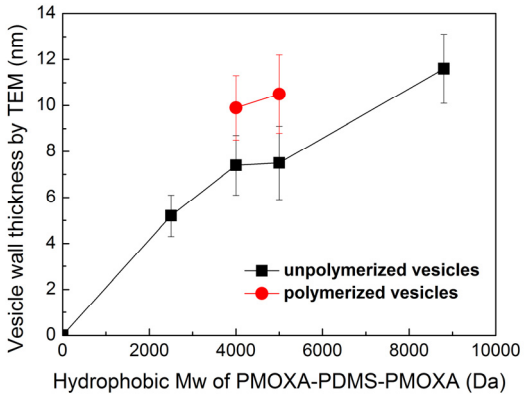

Figure 3. Relationship between the molecular weight of the hydrophobic PDMS block in the ABA triblock copolymers and the thickness of the hydrophobic layer in the vesicle membrane (vesicle wall thickness). The vesicle wall thicknesses were measured from TEM images by using Photoshop software. 10 points were randomly selected for each sample. Values are represented with the mean ± standard deviation (n = 10).

The vesicle wall thickness is greatly influenced by the molecular weight of the hydrophobic block of PDMS in the PMOXA-PDMS-PMOXA. Figure 3 shows the correlation between the molecular weight of the hydrophobic block and the vesicle wall thickness measured from TEM. It can be seen that, vesicle wall thickness increases from 5.2 nm to 11.6 nm when the molecular weight of the hydrophobic block PDMS increases from 2500 to 8800. A longer hydrophobic chain length leads to a thicker membrane wall and a higher packing density due to chain entanglement, which is consistent with other reports [34]. In addition, the triblock copolymers P_{4000} and P_{5000} have methacrylate end groups that allow for a UV light-induced polymerization. After UV light exposure,

the methacrylate end groups distributed at the vesicle surface will be polymerized with neighbouring methacrylate end groups and form a covalent bond shell on the vesicle surface, which will enhance the mechanical stability of vesicles. In Figure 3, the red points refer to the wall thickness of vesicles that are formed from methacrylate-copolymers after UV exposure. It is noted that for vesicles prepared from methacrylate-copolymers, P_{4000} and P_{5000}, vesicle wall thickness increases after UV polymerization of the methacrylate end groups as compared to vesicles without or before polymerization.

3.2. Vesicle wall thickness and AqpZ permeability

The hydrophobic thickness of the polymer vesicles, as shown in Figure 3, is thicker than that of lipid bilayers, which is 3 nm [36]. When AqpZ is reconstituted into polymer vesicles, there is hydrophobic mismatch between the hydrophobic length of the AqpZ and the hydrophobic thickness of the membrane, as shown in Figure 4. It has been reported that the membrane protein with hydrophobic mismatch towards the neighbouring bilayer will distort the bilayer at the interface, resulting in the bilayer morphology not being aligned correctly with the protein [37]. It has also been reported that the elastic lipid chain distortions are insufficient to compensate fully for the mismatch [38], and the structure and dynamics of protein might change due to this hydrophobic mismatch [39,40]. The stretched or compressed structure of AqpZ might affect water transport behavior of the water channels. In this work, the permeability of AqpZ that reconstituted in these polymers was therefore investigated through the vesicle permeability using stopped-flow spectroscopy.

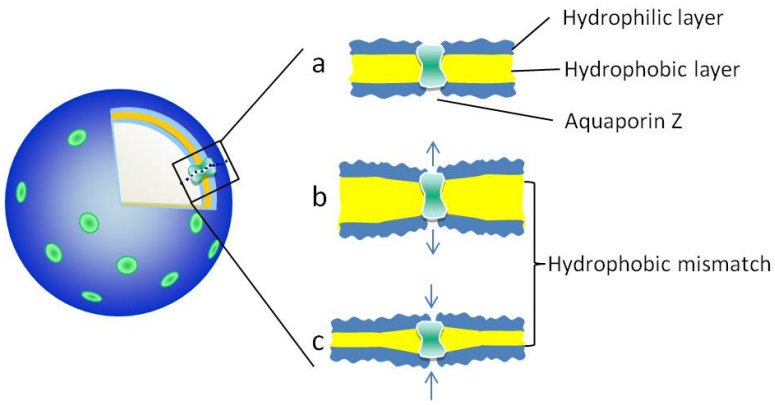

Figure 4. Schematic diagram of hydrophobic mismatch between the reconstituted AqpZ and the hydrophobic layer of the vesicle membrane.

Figure 5 shows examples of the light scattering intensity curves for blank polymersomes (Figure 5a) and proteopolymersomes (Figure 5b). It can be observed from Figure 5a that with increasing hydrophobic chain length, vesicle size responds slower to the osmotic pressure. When the hydrophobic chain length is above 5000 Da, vesicle size almost does not respond to the osmotic pressure, indicating an extremely slow water diffusion speed across the thick hydrophobic wall and a negligible water permeability of the blank polymersomes. From Figure 5b, it can be observed that all AqpZ reconstituted vesicles shrink more quickly than the blank vesicles under the osmotic pressure. This proves that AqpZ has been successfully reconstituted to maintain its water transport

functionality in these polymer vesicles. According to Figure 3, vesicle wall thickness ranges from 5.2 to 11.6 nm, which is much thicker than the lipid bilayer. The stopped-flow results gave us confidence that the hydrophobic mismatch, which is less than 9 nm, will not lead to AqpZ misfolding or denaturation.

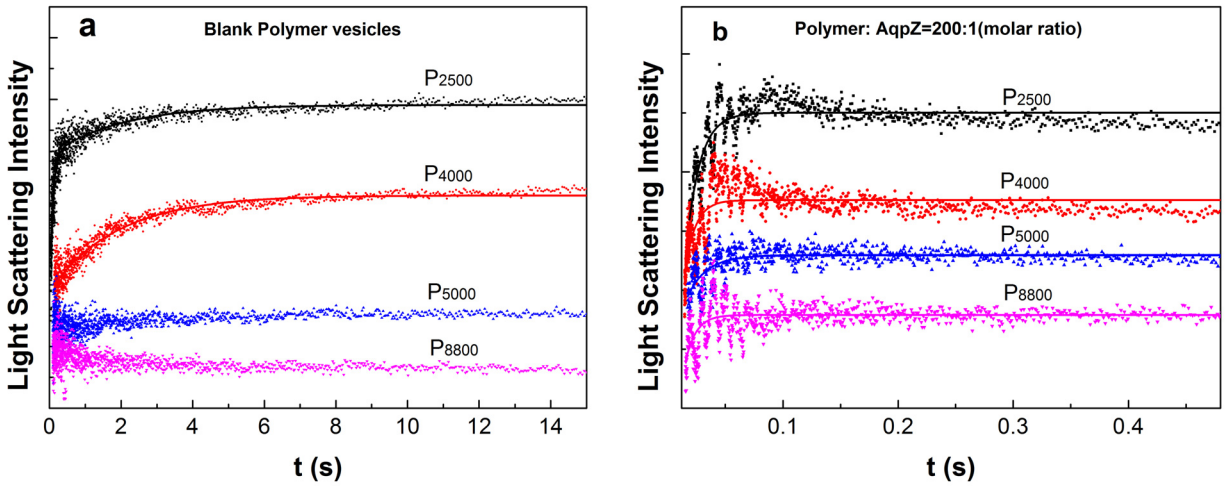

Figure 5. Water permeability of the vesicles determined by a stopped-flow spectroscopy. The increase in the light scattering signal represents a reduction in vesicle size due to water efflux from the vesicle to the solution. The data were exponentially fitted by equation (1). The solid lines represent fitting curves. (a) The relative light scattering signals of blank vesicles without AqpZ incorporation; (b) The relative light scattering signals of AqpZ-reconstituted vesicles at a protein–polymer molar ratio of 1:200.

Figure 6 shows permeabilities for both types of vesicles (Figure 6a) and each AqpZ unit in proteopolymersomes (Figure 6b). In this work, the molecular weight of the hydrophobic block PDMS ranges from 2500 to 8800 Da. Correspondingly, vesicle wall thickness ranges from 5.2 nm to 11.6 nm. A stretched AqpZ structure might take place due to the hydrophobic mismatch between the AqpZ protein and a thick hydrophobic layer of the vesicle membrane. In order to investigate whether the stretched structure of AqpZ affected the water transport behavior of the water channels, we calculated the water permeability of each AqpZ unit (Pa) in these vesicles. The Pa value ranges from 6.9 to 14 × 10^{-14} cm^3 s^{-1} which is consistent with Verkman's results (from 6 to 24 × 10^{-14} cm^3 s^{-1}) [41], indicating that the hydrophobic mismatch, in our experiment range, will not lead to AqpZ misfolding or denaturation. Moreover, from Figure 6b, we find that a thicker vesicle wall leads to a larger Pa value, indicating that the hydrophobic mismatch in our experiment range enhances the water permeability of the AqpZ channel. The reason could be due to the water channel being distorted and expanded to a small extent, forming a "stretched structure" of AqpZ. Further evidence will be needed to confirm this hypothesis of a stretched AqpZ structure in the polymer bilayers.

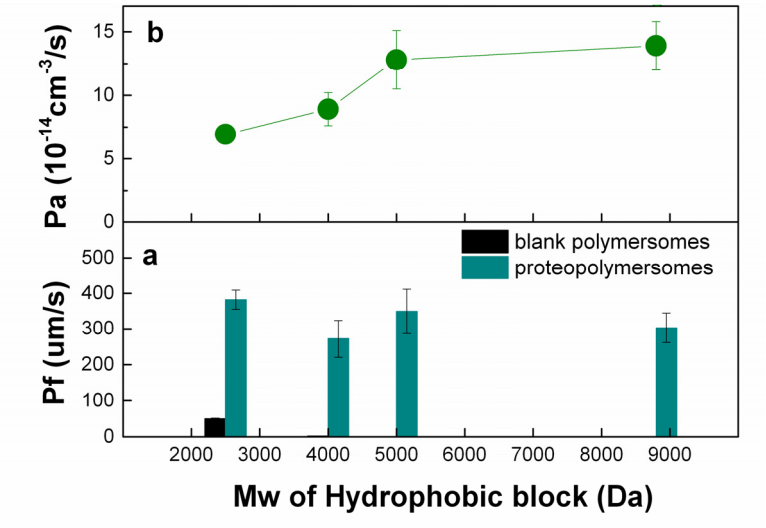

Figure 6. (a) Permeability coefficient (Pf) of vesicles, and (b) permeability of each AqpZ unit (Pa). Pf and Pa are determined by stopped-flow spectroscopy. The light scattering signals from stopped-flow were exponentially fitted by equation (1). Pf and Pa are calculated by using equation (2) and equation (3), respectively. All the experiment data have been repeated 3 times. Values represent the mean ± standard deviation (error bars) with n = 3.

3.3. Hydrophobic mismatch vs. Arrhenius activation energies for water molecule across the vesicle

To investigate the activation energies for water transport in both the polymer bilayers and the AqpZ channels, stopped-flow spectroscopy and light scattering analysis were performed at various temperatures ranging from 278 K to 303 K. Figure 7 was plotted using the derived ln k values against the inverse temperature values, 1/T, where k is the initial rate constant (s^{-1}) of the light scattering intensity signal, and T is the temperature. The observed trends for the ln k values of the blank polymer vesicles and AqpZ-reconstituted polymer vesicles to the variation in experimental temperatures were consistent for all the ABA copolymers used, and exhibited similar linearly decreasing trends. When temperature increases, more heat energy is provided to the water molecules present. The heat energy gained by the water molecules gets converted to kinetic energy, leading to an increase in the rate of transport of the water molecules across the membrane through the AqpZ channels. In addition, higher temperature provides higher kinetic energy to the water molecules, leading to greater frequency and impact of the water molecules against the bilayer structure. Therefore, this gives rise to a greater number of water molecules passing through the bilayer structure through the pores present between the polymers, without going through AqpZ proteins.

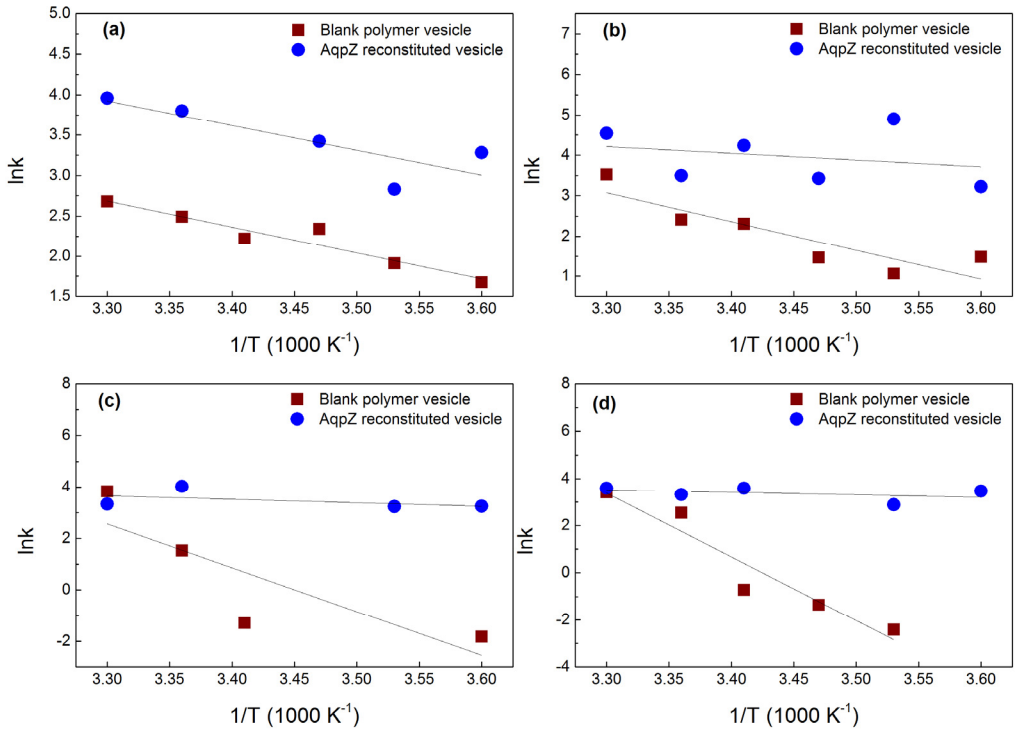

Figure 7. Arrhenius plots for calculation of activation energy for osmotic transport of water across AqpZ-reconstituted polymer vesicles and blank polymer vesicles. In AqpZ-reconstituted vesicles, the protein-polymer molar ratio was 400:1. Polymers used in these vesicles were (a) P_{2500}, (b) P_{4000}, (c) P_{5000} and (d) P_{8800}. All the experimental data have been repeated 3 times. Values represent the mean value.

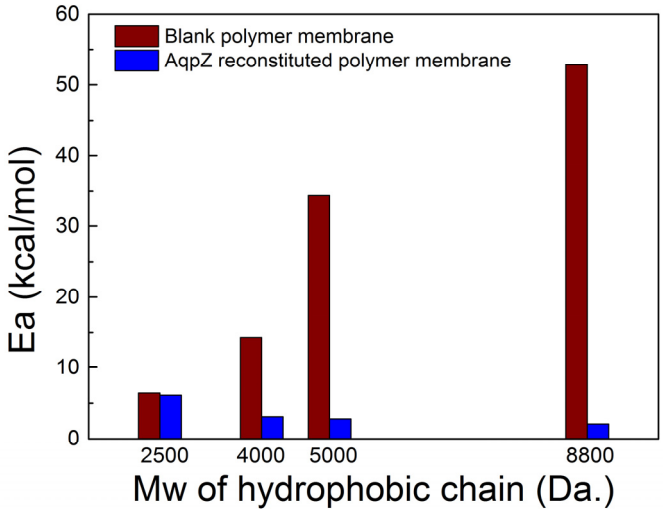

Figure 8. Arrhenius activation energy for osmotic transport of water across AqpZ-reconstituted polymer membranes and blank polymer membranes with various hydrophobic chain lengths.

As shown in Figure 8, the calculated Arrhenius activation energies for blank polymer bilayers ranges from 6.4 to 52.8 kcal/mol, which is consistent with the reported activation values for water transport across polymer membranes [42]. The high Arrhenius activation energies of blank polymer vesicles indicate that the water transport through polymer bilayers is based on a diffusion-driven mechanism. It can also be observed that higher Arrhenius activation energies were obtained from the polymer vesicles with higher hydrophobic molecular weight, compared to those polymer vesicles with lower hydrophobic molecular weight. The denser packing of the longer hydrophobic chain and the thicker membrane hydrophobic thickness form a larger barrier for diffusion, requiring higher activation energies for water molecules passing through. Arrhenius activation energies for AqpZ reconstituted polymer vesicles range from 2.1 to 6.1 kcal/mol. These lower Arrhenius activation energies indicate that water transport across the AqpZ reconstituted vesicles is channel-mediated. Borgnia et al. reported that the activation energy for AqpZ channel is 3.7 kcal/mol in proteoliposomes [12] and thus our results are comparable to the reported value. In addition, when AqpZ were reconstituted into block copolymers with longer hydrophobic chains, a lower Arrhenius activation energy was required for water molecules to pass through the AqpZ channel. It again implies that the structure of AqpZ channel might be stretched to some-extent due to the hydrophobic mismatch, leading to a wider channel for the water molecule to pass through. To confirm this hypothesis, further investigations using x-ray crystallography, NMR spectroscopy and molecular dynamics simulation will be needed.

3.4. pH value of environmental solution vs. AqpZ permeability

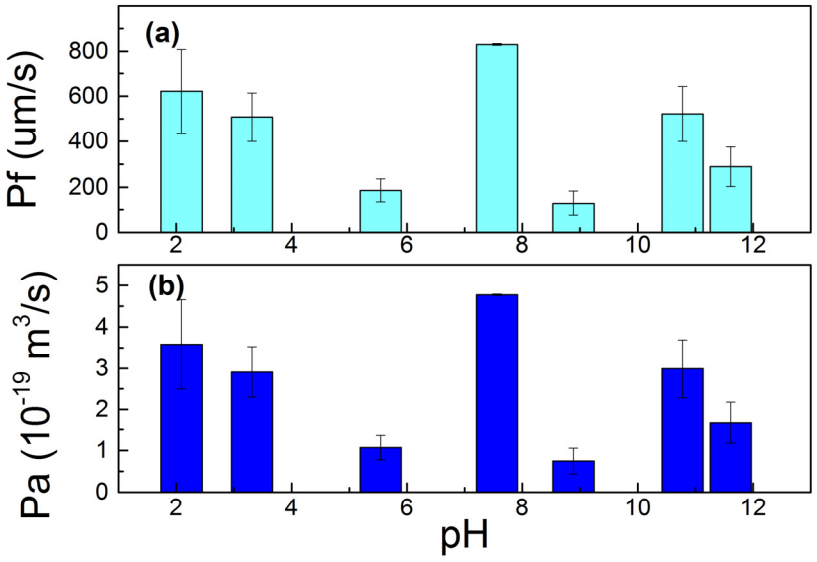

Figure 9. (a) Vesicle permeability coefficient (Pf), and (b) permeability of each AqpZ unit (Pa) versus pH value of the buffer solution. Proteopolymersomes were made from P_{4000}. The polymer to protein molar ratio was 400:1. All the experiment data have been repeated 3 times. Values represent the mean ± standard deviation (error bars) with n =3.

Figure 9a shows the permeability coefficients of the AqpZ-reconstituted P_{4000} vesicle in buffer solutions with different pH values. The highest Pf appears near neutral conditions when the pH is 7.5.

With increasing concentration of H^+, the Pf greatly decreased at pH of 5.5, and increased again in the strongly acidic environment with pH less than 3.5. On the other hand, with increasing concentration of OH^- in the vesicle solution, the Pf value also greatly decreased at pH of 8.9 and followed by a slight increase at the strongly basic environment with a pH of more than 10. Further, we calculated the osmotic permeability of AqpZ channel (Pa) based on the Pf value. As shown in Figure 9b, the Pa versus the pH shows the same trend as the vesicle permeability coefficient (Pf). This shows that the water filtration mechanism of AqpZ is significantly affected by the ions of H^+ and OH^-.

The observed trends for the regulation in the osmotic permeability of the AqpZ-ABA vesicles (Figure 9a) and the individual AqpZ proteins (Figure 9b) are similar with respect to the variation in pH. The tendency of the osmotic permeability to decrease with increasing pH values may be attributed to the structure of AqpZ. Near the constriction of the AqpZ hydrophobic channel, there are histidine (H) and arginine (R) residues present in the AqpZ monomer loops at positions H180 and R195 respectively that provide the positive charges required in the water transport mechanism of AqpZ [14,15]. Histidine has an overall pI value of 7.6 with their imidazole side chains having a pKa of about 6.0, while arginine has an overall pI value of 10.8 with their guanidinium side chains having a pKa of 12.5. Hence, the positive charges present on the residues will change with pH due to the effects of protonation.

The change in the protonation status of the –COOH terminal group of the amino acid residues as pH changes, may have an effect on the water-pore interaction and the formation of the single file configuration of water molecules passing through the AqpZ channel. Thus AqpZ water transport efficiency was affected since the separation capabilities of AqpZ stems from the formation of the single file of water molecule, which prohibits proton translocation and is dependent on the positive charges present at positions H180 and R195 [14,15].

4. Conclusion

There is an increasing pressure to innovate cheaper forms of membrane technologies to address the issue of water scarcity. Biomimetic membrane technologies utilizing aquaporin is an attractive alternative that can carry out filtration at high capacities using a lower pressure gradient. For AqpZ to be exploited successfully in membrane filtration, an understanding of the factors that influence the osmotic permeability of AqpZ is critical. This study investigated the influences of factors such as pH, temperature, crosslinking and the molecular structure of the ABA tri-block copolymers (PMOXA-PDMS-PMOXA) in which the AqpZ was incorporated, on the osmotic permeability of AqpZ. Results show that the molecular structure of PMOXA-PDMS-PMOXA significantly alters the vesicle morphology and aquaporin functionality. Block copolymers with longer hydrophobic chains form vesicles with thicker hydrophobic walls, resulting in larger hydrophobic mismatch between the protein and the bilayer membrane. The stopped flow results show that the osmotic permeability of AqpZ has improved when reconstituted in a bilayer with a larger hydrophobic thickness. The Arrhenius activation energies for water transport across the AqpZ channel show a decreasing trend with increasing hydrophobic thickness of the bilayers, indicating a “stretched structure” of the AqpZ when encountering a lengthening hydrophobic mismatch. In addition, we found that the water filtration mechanism of the AqpZ protein is significantly affected by the ionic concentrations of H^+ and OH^-. The individual AqpZ exhibits the highest osmotic permeability in neutral solution. The ApqZ osmotic permeability decreased with either increasing concentrations of H^+, or increasing concentrations of OH^-.

Acknowledgements

This work was financially supported by Singapore's National Research Foundation (NRF) through the Environment and Water Industry Programme Office (EWIPO) EWI projects, 1102-IRIS-13-01 and 1102-IRIS-13-02 as well as the NUS grant R706000022279. The authors would like to thank Prof. T. S. Chung, Drs Q. Lin, H. Wang, H. Zhou, L. Wang for their suggestions and help with this work.

Conflict of Interest

All authors declare no conflicts of interest in this paper.

References

1. Kumar M, Grzelakowski M, Zilles J, et al. (2007) Highly permeable polymeri membranes based on the incorporation of the functional water channel protein Aquaporin Z. *PNAS* 104: 20719–20724.
2. Service RF (2006) Desalination freshens up. *Science* 313:1088–1090.
3. Tal A (2006) Seeking sustainability: Israel's evolving water management strategy. *Science* 313: 1081–1084.
4. Discher BM, Won YY, Ege DS, et al. (1999) Polymersomes: tough vesicles made from diblock copolymers. *Science* 284:1143–1146.
5. Calamita G, Kempf B, Rudd KE, et al. (1997) The aquaporin-Z water channel gene of Escherichia coli: Structure, organization and phylogeny. *Biology of the Cell* 89: 321–329.
6. Calamita G, Bishai WR, Preston GM, et al. (1995) Molecular cloning and characterization of AqpZ, a water channel from Escherichia coli. *J Biol Chem* 270: 29063–29066.
7. Scheuring S, Ringler P, Borgnia M, et al. (1999) High resultion AFM topographs of the Escherichia coli water channel aquaporin Z. *EMBO J* 18: 4981–4987.
8. Gorin MB, Yancey SB, Cline J, et al. (1984) The major intrinsic protein (MIP) of the bovine lens fiber membrane: Characterization and structure based on cDNA cloning. *Cell* 39: 49–59.
9. Ishibashi K, Kuwahara M, Gu Y, et al. (1997) Cloning and functional expression of a new water channel abundantly expressed in the testis permeable to water, glycerol and urea. *J Biol Chem* 272: 20782–20786.
10. Soupene E, King N, Lee H, et al. (2001) Aquaporin Z of *Escherichia coli*: Reassessment of Its Regulation and Physiological Role. *J Bacter* 184: 4304–4307.
11. Calamita G, Kempf B, Bonhivers B, et al. (1998) Regulation of the Escherichia coli water channel gene AqpZ. *Proc Natl Acad Sci U S A* 95: 3627–3631.
12. Borgnia MJ, Kozono D, Calamita G, et al. (1999) Funcation Reconstitution and Characterization of AqpZ, the E. coli Water Channel Protein. *J Mol Biol* 291: 1169–1179.
13. Kozono D, Yasui M, King LS, et al. (2002). Aquaporin water channels: atomic structure molecular dynamics meet clinical medicine. *J Clin Inves* 109: 1395–1399.
14. Nemeth-Cahalan KL, Hall JE (2000) pH and Calcium Regulate the Water Permeability of Aquaporin 0. *J Biol Chem* 275: 6777–6782.
15. Cahalan K, Kalman K, Hall JE (2004) Molecular Basis of pH and Ca2+ Regulation of Aquaporin Water Permeability. *J Gen Physiol* 123: 573–580

16. Zhou W, Jones SW (1996) The effects of external pH on calcium channel currents in bullfrog sympathetic neurons. *Biophys J* 70: 1326–1334
17. Gonen T, Walz T (2006) The structure of aquaporins. *Q Rev Biophys* 39: 361–396.
18. Chaumont F, Moshelion F, Daniels MJ (2005) Regulation of plant aquaporin activity. *Biol Cell* 97: 749–764.
19. Tong J, Canty JT, Briggs MM, et al. (2013) The water permeability of lens aquaporin-0 depends on its lipid bilayer environment. *Exp Eye Res* 113: 32–40.
20. Andersen OS, Bruno MJ, Sun H, et al. (2007) Single-molecule methods for monitoring changes in bilayer elastic properties. *Meth Mol Biol* 400: 543–570
21. Hong H, Tamm LK (2004) Elastic coupling of integral membrane protein stability to lipid bilayer forces. *Proc Natl Acad Sci U S A* 101: 4065–4070.
22. Nyholm TK, Ozdirekcan S, Killian JA (2007) How protein transmembrane segments sense the lipid environment. *Biochemistry* 46: 1457–1465.
23. Phillips R, Ursell T, Wiggins P, et al. (2009) Emerging roles for lipids in shaping membrane-protein function. *Nature* 459: 379–385.
24. Yuan C, O'Connell RJ, Jacob RF, et al. (2007) Regulation of the gating of BKCa channel by lipid bilayer thickness. *J Biol Chem* 282: 7276–7286.
25. Dumas F, Tocanne JF, Leblanc G, et al. (2000) Consequences of hydrophobic mismatch between lipids and melibiose permease on melibiose transport. *Biochem* 39: 4846–4854.
26. Perozo E, Kloda A, Cortes DM, et al. (2002) Physical principles underlying the transduction of bilayer deformation forces during mechano senditive channel gating. *Nat Struct Biol* 9: 696–703.
27. Xie W, He F, Wang B, et al. (2013) An aquaporin-based vesicle-embedded polymeric membrane for low energy water filtration. *J Mater Chem A* 1: 7592–7600.
28. Wang H, Chung TS, Tong YW, et al. (2011) Preparation and characterization of pore-suspending biomimetic membranes embedded with Aquaporin Z on carboxylated polyethylene glycol polymer cushion. *Soft Matter* 7: 7274–7280.
29. Wang H, Chung TS, Tong YW, et al. (2012) Highly permeable and selective pore-spanning biomimetic membrane embedded with aquaporin Z. *Small* 8: 1185–1190, 1125.
30. Duong PHH, Chung TS, Jeyaseelan K, et al. (2012) Planar biomimetic aquaporin-incorporated triblock copolymer membranes on porous alumina supports for nanofiltration. *J Membr Sci* 409: 34–43.
31. Zhong PS, Chung TS, Jeyaseelan K, et al. (2012) Aquaporin-embedded biomimetic membranes for nanofiltration. *J Membr Sci* 407: 27–33.
32. Savage DF, Egea PF, Colmenares YR, et al. (2013) Architecture and selectivity in aquaporins: 2.5A X-Ray Structure of Aquaporin Z. *PLoS Biol* 1: 334–340.
33. Nielsen CH (2009) Biomimetic membranes for sensor and separation applications. *Bioanal Chem* 395: 697–718.
34. Discher DE, Eisenberg A(2002) Polymer vesicles. *Science* 297: 967–973.
35. Ahmed F, Photos PJ, Discher DE (2006) Polymersomes as viral capsid mimics. *Drug Develop Res* 67: 4–14.
36. Lewis BA, Engelman DM (1983) Lipid Bilayer Thickness Varies Linearly with Acyl Chain Length in Fluid Phosphatidylcholine Vesicles. *J Mol Biol* 166: 211–217.
37. Dave PC, Tiburu EK, Damodaran K, et al. (2004) Investigating Structural Changes in the Lipid Bilayer upon Insertion of the Transmembrane Domain of the Membrane-Bound Protein Phospholamban Utilizing ^{31}P and ^{2}H Solid-State NMR Spectroscopy. *Biophys J* 86: 1564–1573.

38. Marsh D (2008) Energetics of Hydrophobic Matching in Lipid-Protein Interactions. *Biophys J* 94: 3996–4013.
39. Xu Q, Kim M, David Ho KW, et al. (2008) Membrane Hydrocarbon Thickness Modulates the Dynamics of a Membrane Transport Protein. *Biophys J* 95: 2849–2858.
40. He F, Tong YW (2014) A mechanistic study on amphiphilic block co-polymer poly(butadiene-b-(ethylene oxide)) vesicles reveals the water permeation mechanism through a polymeric bilayer. *RSC Adv* 4: 15304–15313.
41. Yang B, Verkman AS (1997) Water and Glycerol Permeabilities of Aquaporins 1–5 and MIP Determined Quantitatively by Expression of Epitope-tagged Constructs in Xenopus Oocytes. *J Biol Chem* 272: 16140–16146.
42. Mehdizadeh H, Dickson JM, Eriksson PK (1989) Temperature effects on the performance of thin-film composite, aromatic polyamide membranes. *Ind Eng Chem Res* 28: 814–824.

AIMS Press